

## **Modelling of tritium retention and target lifetime of the ITER divertor**

A. Kirschner<sup>1</sup>, S. Droste<sup>1</sup>, D. Borodin<sup>1</sup>, V. Philipps<sup>1</sup>, U. Samm<sup>1</sup>, G. Federici<sup>2</sup>, J. Roth<sup>3</sup>

<sup>1</sup>*Institut für Plasmaphysik, Forschungszentrum Jülich GmbH, EURATOM Association, Trilateral Euergio Cluster, 52425 Jülich, Germany,*

<sup>2</sup>*ITER JWS Garching Co Center, Boltzmannstr. 2, 85748 Garching, Germany*

<sup>3</sup>*Max-Planck Institut für Plasmaphysik, EURATOM Association, Boltzmannstr. 2, 85748 Garching, Germany*

Erosion, deposition and transport of eroded material in the divertor of ITER are modelled with the Monte Carlo impurity transport code ERO taking into account chemical erosion, physical sputtering, enhanced erosion of redeposited carbon and beryllium deposition. With increasing exposure time continuous deposition of beryllium leads to reduced carbon erosion along the divertor plates. The limit of discharges possible from the estimated long-term tritium retention ranges between 440 using an effective sticking of unity for redeposited hydrocarbons and 380 for an effective sticking of zero. The lifetime of the divertor plates is less critical than tritium-retention, in the worst case about 7000 ITER discharges. Erosion due to transient heat loads (ELMs or disruptions) are not yet included in the modelling.

### **Introduction**

In the current design of ITER, carbon fibre composites (CFC) are foreseen for the divertor target plates where the highest heat loads are expected. The advantage of non-melting of graphite materials opposes their strong erosion due to chemical formation of hydrocarbon molecules even at low plasma temperatures. Extrapolations from current experiments to ITER indicate a critical amount of tritium retention due to co-deposition. However, experimental data are based on full-carbon clad devices whereas in ITER beryllium is foreseen for the main wall and tungsten for the baffles and the dome. No experimental data exist for this material choice and extrapolation must therefore base on a reasonable understanding of the processes determining the fuel retention taking into account the ITER material mix.

This contribution presents ERO modelling of erosion and deposition along the divertor target plates taking into account a uniform background beryllium influx of 1% relative to the incoming deuterium ion flux. Eroded particles are followed through the divertor plasma until they are redeposited at the divertor plates or escape the plasma volume considered in the code. Particles not locally redeposited are assumed to form carbon-layers at remote areas leading to long-term tritium retention. The chemical erosion yield by deuterium impact (ions and atoms) is calculated using the new semi-empirical "Roth" formula depending on the incoming deuterium flux density, surface temperature and deuterium impact energy [1]. The chemical erosion of redeposited carbon species is assumed to be enhanced by a factor of ten compared to the erosion of graphite [2]. Physical sputtering is caused by background deuterium and beryllium ions and also by eroded impurities.

### **Input parameter for the ERO modelling**

The plasma background parameters for the ERO calculations are taken from B2-EIRENE calculations [3]. Figure 1 shows profiles of the deuterium ion and atom flux density, electron density and temperature as function of the distance  $d$  along the divertor plates. The distance  $d=0$  (dotted lines) corresponds to the location of the separatrix.

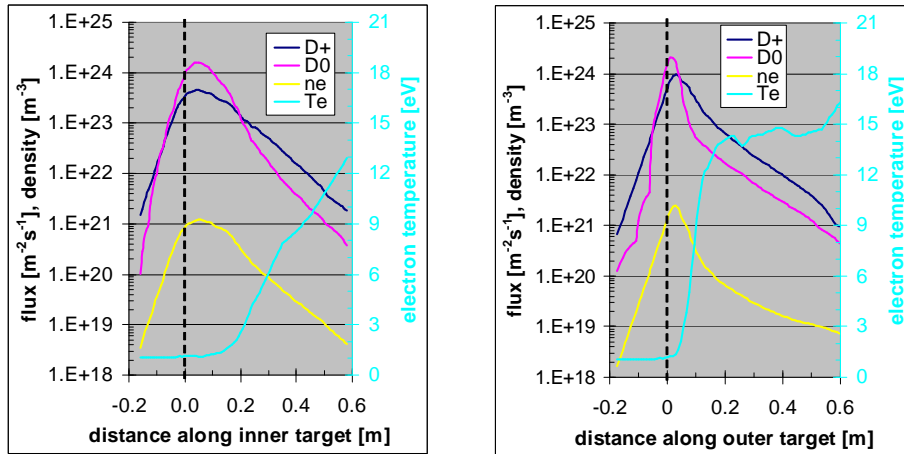


**Figure 1** Deuterium ion and atom flux, electron density and temperature along inner (left) and outer (right) divertor target plate (from B2-EIRENE).

Using these plasma parameters, chemical and physical erosion yields as shown in figure 2 are calculated. For simplicity, the figures show only the erosion by deuterium ions whereas a similar picture arises from erosion due to deuterium atoms. Figure 2 shows also the parameters determining the chemical and physical sputtering yield, i.e. the incoming deuterium ion flux, the surface temperature and the deuterium ion impact energy. The surface temperature is calculated for a CFC target of 10mm thickness with a thermal conductivity representing average operations conditions.

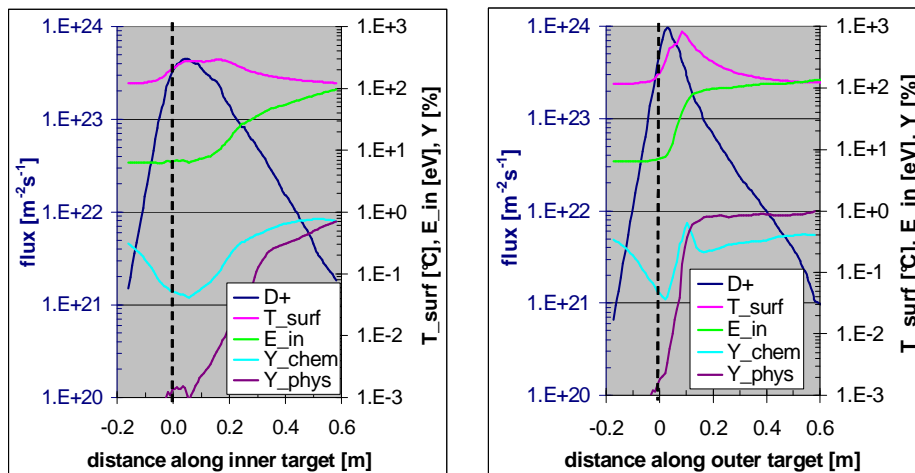


**Figure 2** Profiles of deuterium ion flux, surface temperature, impact energy, chemical erosion and physical sputtering yield along the divertor plates (left – inner, right – outer divertor).

Coming along the target from the private flux region (PFR, negative distances from the separatrix) to the scrape-off-layer (SOL), the chemical erosion yield decreases reaching a minimum of about 0.04% for the inner and outer divertor at the location of the highest flux density. In the inner divertor, the yield increases continuously along the target moving into the SOL reaching a value of about 0.8%. In the outer divertor, a local maximum is reached at the position where the surface temperature reaches about 600°C, but the yield decreases then due to the decrease of the surface temperature before it increases again further into the SOL up to a value of about 0.4%. Physical sputtering only occurs in the SOL whereas in the PFR the deuterium impact energy is too low (yield smaller than ~0.001% in inner and outer PFR). Physical sputtering is more important in the outer divertor SOL where the yield reaches about 1% for distances from the separatrix larger than 20cm whereas a comparable yield in the inner divertor is reached at a distance of about 60cm.

## ERO modelling results

**Dynamic erosion behaviour:** At first, an effective sticking of zero for hydrocarbons returning to the divertor plates is assumed. The influence of the effective sticking will be discussed later in the context of target lifetime and tritium retention.

The modelling starts with a pure graphite (c) surface. The graphite erosion rate integrated over the divertor plates first decreases with exposure time due to deposition of beryllium and then approaches a constant equilibrium value. The integrated erosion rate of all redeposited carbon (cr) increases from zero to a maximum after which it also decreases until it reaches a constant value in equilibrium. Figure 3a shows the erosion profile along the inner divertor plate of the “pure” graphite at the beginning and of the sum of graphite and redeposited carbon in equilibrium. It is seen that the initial graphite erosion around the separatrix is suppressed leading in equilibrium to an erosion profile that is peaked more inside the SOL compared to the original broader erosion distribution. In equilibrium the integrated total carbon (graphite plus redeposited carbon) erosion rate in the inner divertor is decreased by a factor of  $\sim 2$  compared with the beginning and by a factor of  $\sim 3$  in the outer divertor. Figure 3b shows the surface concentration profiles along the inner divertor plate for carbon, redeposited carbon and beryllium in equilibrium. Between  $d=-0.03\text{m}$  and  $d=0.15\text{m}$  a net deposition zone for beryllium ( $c_{\text{Be}}=1$ ) develops leading to a complete suppression of carbon erosion. Outside this zone the carbon concentration in the surface is below 1. Redeposited carbon cr is found mainly between  $d=0.15\text{m}$  and  $0.6\text{m}$  with a maximum concentration of  $\sim 0.2$ . Similar profiles develop along the outer divertor plate while the zone of net beryllium deposition extends less far into the SOL with a higher maximum concentration of redeposited carbon (about 0.3).

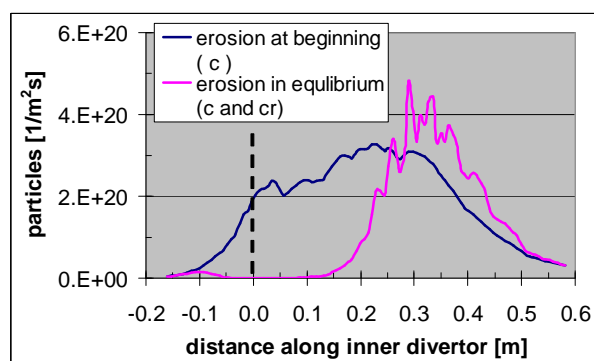


**Figure 3a** Erosion profile along inner divertor plates of graphite (c) at the beginning and of graphite plus redeposited carbon (c+cr) in equilibrium.

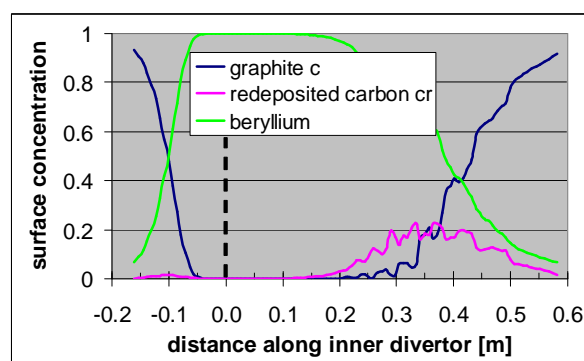


**Figure 3b** Surface concentration along inner divertor plates of graphite (c), redeposited carbon (cr) and beryllium (be) in equilibrium.

**Divertor target lifetime and long-term tritium retention:** In equilibrium and with the assumption of zero effective sticking for hydrocarbons about 94% of eroded carbon is redeposited at the inner divertor plate. The resulting net-deposition profile of carbon (redeposited carbon cr minus erosion of graphite c minus erosion of redeposited carbon cr) for the inner divertor plate is shown in figure 4 after 10s simulation time. After a net-erosion zone in the PFR and at the beginning of the SOL a net deposition zone develops reaching a maximum deposition at  $d=0.25\text{m}$ . Going further into the SOL, a net-erosion zone develops again with a maximum erosion at  $d\sim 0.4\text{m}$ . Adding the beryllium deposition strongly changes the picture. Only at distances larger than  $d\sim 0.45\text{m}$  net-erosion occurs whereas the other

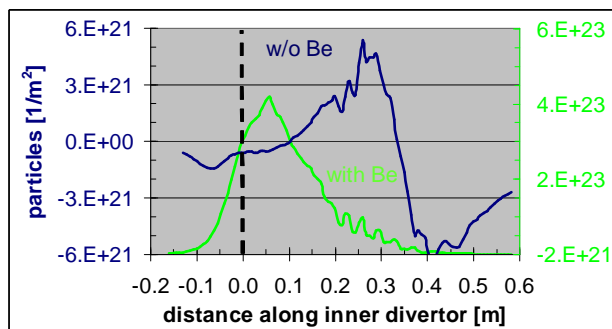


**Figure 4** Profile of net-carbon erosion/deposition after 10s and same profile but with beryllium deposition added.

erosion zones are turned into net-deposition areas. At the location of maximum net-erosion (around  $d=0.5\text{cm}$ ) an erosion rate of about  $1.8\text{ nm/s}$  is estimated, which would yield a lifetime for the inner target (erosion of  $0.5\text{cm}$ ) of about 7000 shots with a shot length of 400s. If an effective sticking of 1 for hydrocarbons is assumed, the carbon redeposition fraction is increased to about 97% with a similar increase of the target lifetime. In the outer divertor the maximum net-erosion is about a factor of 5 smaller than in the inner divertor and the redeposition is slightly larger (for  $S_{\text{eff}}=0$ ). Both leads to an increased target lifetime compared to the inner divertor plate.

The long-term tritium retention is assumed to be caused by eroded carbon not redeposited locally on the divertor target plates. In equilibrium the amount of locally redeposited carbon and therefore tritium does not change with exposure time (erosion equals redeposition). However, not-locally deposited species are transported mainly to the PFR and further to the dome region where the formation of tritium-containing carbon layers is expected. Assuming a T/C ratio of 0.5 results in estimated tritium retention rates as shown in table 1. The retention rates for the outer divertor are slightly larger than for the inner. However, significant tritium retention will also occur in the beryllium layers. Assuming  $(D+T)/\text{Be}=0.01$  would lead to an

Effective sticking of hydrocarbons	Inner divertor	Outer divertor
$S_{\text{eff}} = 0$	0.3mg T/s	0.5mg T/s
$S_{\text{eff}} = 1$	0.2mg T/s	0.3mg T/s

**Table 1** Estimated long-term tritium retention rate in remotely formed carbon layers.

additional rate of  $1.5\text{mg T/s}$  (inner and outer divertor). Altogether the maximum number of discharges after which the allowed in-vessel tritium inventory of 350g is reached, would be 380 for an effective sticking  $S_{\text{eff}}=0$  for hydrocarbons and increases to 440 for  $S_{\text{eff}}=1$ .

## Conclusions

The modelling shows that the long-term tritium retention is much more critical than target lifetime. Calculations of T retention based on the erosion and redeposition of carbon using recently developed erosion yields and taking into account a Be influx in the divertor of 1% yield 380 - 440 ITER discharges before the tritium limit of 350g is reached (depending on assumptions on re-erosion of redeposited hydrocarbons). However, one has to keep in mind that the influence of transient heat loads such as ELMs or disruptions is not considered here. The beneficial effect of reduction of carbon erosion due to the coverage with beryllium could vanish if the beryllium layers do not withstand such heat loads. In addition, deposition of carbon inside the gaps between the castellated divertor plates will possibly increase the long-term tritium retention.

[1] J. Roth et al., J. Nucl. Mat. 337-339 (2005) 970

[2] A. Kirschner et al., J. Nucl. Mat. 328 (2004) 62

[3] G. Federici et al., J. Nucl. Mat. 313-316 (2003) 11